METHODS AND APPLICATIONS OF ANALYSIS.
Vol. 10, No. 2, pp. 329–346, June 2003

010

LEVEL SET METHOD FOR SHAPE OPTIMIZATION OF PLATE PIEZOELECTRIC PATCHES *

JIANYING ZHANG†

Dedicated to Professor Stanley Osher's 60th Birthday

Abstract. We consider a vibrating system with piezoelectric patches whose minimum vibration frequency is to be minimized subject to some constraint on the patch geometry. A numerical scheme is constructed using the level set method devised in [12] and the projected gradient method devised in [14] to optimize the patch geometry. An integral equation approach introduced in [4, 17, 20, 21] is also presented for the computation of the corresponding eigenvalue problem.

Introduction. A piezoelectric material can respond to mechanical forces/pressures and generate an electric charge/voltage. This piezoelectric phenomenon is called the *direct piezoelectric effect*. On the other hand, an electric charge/field applied to the material induces mechanical stresses or strains, and this phenomenon is called the *converse piezoelectric effect*. In active piezoelectric structures, the *direct* effect is used for structural measurements while the *converse* effect is used for active vibration controls of the continua.

In recent years, piezoelectric materials are being used increasingly in noise control [5, 6], vibration control [3, 8] and shape control [9, 10]. They have been effectively employed in areas such as acoustics for noise cancellations with applications to reduce interior noise in aircraft, aerodynamics to adjust wing surfaces and electronics where they are used in the reading heads in videocassette recorders and in compact discs as positioning devices. Another application is in adaptive structures for shape control by piezo-actuation. Also adaptive materials and structures are presently being used in a variety of applications involving static control such as robotic and space structures. One of the important issues in the use of piezo actuators is their optimal deployment to minimize their weight and enhance system performance. In many applications, the piezo materials are used in the form of several patches in order to provides flexibility in choosing their locations which can be optimized to improve the effective of the control [2].

This work concerns a closed-loop displacement feedback control of a thin rectangular plate reinforced with a sensor patch and an actuator patch. The sensor senses the bending strains of the plate and generates a signal which is amplified and sent to the actuator. The actuator then generates a corresponding signal which causes the plate to bend in the opposite direction. The optimal shapes of the patches (under some constraint) are to be determined to minimize the minimum vibration frequency.

We consider the equation of motion, a fourth order hyperbolic equation derived in [19], with simply supported boundary conditions. In the classical approach presented in [20], the modeling equation is converted into a certain integral equation to which a kernel can be determined explicitly. Consequently, the kernel is expressed in terms of the patch shapes by converting the domain integrals over the patches into the corresponding line integrals over their boundaries. Then optimizing the shapes of the patches amounts to optimizing the parameterizations of their boundaries with the admissible set composed of all the reasonable parameters.

*Received December 1, 2002; accepted for publication March 22, 2004.
†Department of Mathematics, 121-1984 Mathematics Road, University of British Columbia, Vancouver, BC, Canada V6T 1Z2 (jyzhang@math.ubc.ca).

However optimizing the parameterizations of the patch boundary is quite limited since only curves with special geometries can be parameterized explicitly. The level set method [12] – considering the varying patch boundaries in a continuous framework as driven by a certain velocity field overcomes this difficulty and allows much more general admissible sets for the optimization. Shape optimization problems are also studied in [1], [11] and [16] in the level set frame work.

The modeling equation presented here involves the biharmonic operator and a term that is singular on the free boundary. Theoretical issues concerning the existence and uniqueness of the minimizer are not yet completed. However, our numerical observation provides positive evidence of the uniqueness.

In the following section, we set up the optimization problem and introduce some notation that will be used in the later presentation. The level set formulation and the detailed numerical scheme are presented in section 2 and 3, respectively. Numerical results are shown in section 4, followed by discussions in section 5.

1. Mathematical formulation of the optimization problem.

1.1. The optimization problem. Consider a thin plate of length a and width b occupying a rectangular domain denoted by

$$U = \{(x, y) : 0 < x < a,\ 0 < y < b\}.$$

Assume that the plate is reinforced with a laminated biaxial piezoelectric actuator patch (occupying $A^e \subset U$) on the top and a laminated biaxial piezoelectric sensor patch (occupying $S^e \subset U$) on the bottom (Which layer serves as a sensor and which serves as an actuator is not crucial).

We first discuss the equation of motion of the plate.

Let $u(x, y, t)$ represent the transverse deflection of the plate. In the absence of mechanical excitations, the equation of motion of the plate with externally applied control moments is given by ([19])

$$\begin{cases} D\Delta^2 u + \rho h \dfrac{\partial^2 u}{\partial t^2} = \alpha L_1[u]\Delta\chi_{A^e} & \text{in } U,\ t > 0 \\ u(x, y, t) = 0 & \text{on } \partial U,\ t > 0 \\ \dfrac{\partial^2 u}{\partial n^2} = 0 & \text{on } \partial U,\ t > 0 \end{cases} \tag{1.1}$$

in which

$$L_1[u] = -c \iint_{S^e} \Delta u$$

and

$$\chi_{A^e} = \begin{cases} 1 & \text{in } A^e \\ 0 & \text{otherwise} \end{cases}$$

with D, ρ, h, α and c being positive physical constants. In particular, ρ is the material density of the plate and h represents the plate thickness.

In the particular case of a rectangular plate, we have

$$\begin{cases} D\Delta^2 u + \rho h \dfrac{\partial^2 u}{\partial t^2} = \alpha L_1[u]\Delta\chi_{A^e} & \text{in } U,\ t > 0 \\ u(x, y, t) = 0 & \text{on } \partial U,\ t > 0 \\ u_{xx}(0, y, t) = u_{xx}(a, y, t) = 0 & \text{for } 0 < y < b,\ t > 0 \\ u_{yy}(x, 0, t) = u_{yy}(x, b, t) = 0 & \text{for } 0 < x < a,\ t > 0. \end{cases} \tag{1.2}$$

The detailed derivation of equation (1.2) is given in [20].

We shall consider the boundary value problem (1.2) and further seek the solution of the form

$$u(x,y,t) = e^{i\lambda t} w(x,y), \tag{1.3}$$

where λ is the plate vibration frequency depending on the shapes of the patches.

Define the following functional

$$I[A^e] = \min_\lambda |\lambda(A^e)|.$$

Our goal is to minimize $I[A^e]$ among suitable patch shapes in a certain admissible set $\mathcal{A}$ with constraint $|A^e| = K$ ($K > 0$ is some fixed constant representing the area of the patch). That is,

$$\text{minimize} \quad I[A^e] \quad \text{among} \quad A^e \in \mathcal{A}, \quad \text{subject to} \quad |A^e| = K.$$

1.2. Reformulation of the optimization problem. Consider the solution in the form of (1.3). By direct computation, $w(x,y)$ satisfies

$$\begin{cases} \Delta^2 w - \dfrac{\alpha}{D} L_1[w] \Delta \chi_{A^e} = \sigma w & \text{in } U \\ w(x,y) = 0 & \text{on } \partial U \\ w_{xx}(0,y) = w_{xx}(a,y) = 0 & \text{for } 0 < y < b \\ w_{yy}(x,0) = w_{yy}(x,b) = 0 & \text{for } 0 < x < a, \end{cases} \tag{1.4}$$

where

$$\sigma = \frac{\lambda^2 \rho h}{D}. \tag{1.5}$$

Denote the linear operator

$$L[w] = \Delta^2 w - \frac{\alpha}{D} L_1[w] \Delta \chi_{A^e}. \tag{1.6}$$

Equation (1.4) then reads

$$\begin{cases} L[w] = \sigma w & \text{in } U \\ w(x,y) = 0 & \text{on } \partial U \\ w_{xx}(0,y) = w_{xx}(a,y) = 0 & \text{for } 0 < y < b \\ w_{yy}(x,0) = w_{yy}(x,b) = 0 & \text{for } 0 < x < a. \end{cases} \tag{1.7}$$

This is an eigenvalue problem in differential equation form. The eigenvalue σ is related to the plate vibration frequency λ via (1.5).

In the case that $\lambda > 0$, the above optimization problem is equivalent to

$$\text{minimize} \quad \min_\sigma \sigma(A^e) \quad \text{among} \quad A^e \in \mathcal{A}, \quad \text{subject to} \quad |A^e| = K.$$

due to (1.5).

1.3. A weak formulation of the eigenvalue problem. Equation (1.7) is understood in the sense of distributions. It is natural to consider a weak solution $w \in H_0^1(U) \cap H^2(U)$. Due to the boundary conditions that w satisfies, we have

$$\begin{aligned}\iint_U \psi \Delta^2 w &= \iint_U \psi \Delta(\Delta w) \\ &= -\iint_U \nabla\psi \cdot \nabla(\Delta w) + \underbrace{\int_{\partial U} \psi \nabla(\Delta w) \cdot dS}_{=0} \\ &= \iint_U \Delta w \Delta\psi - \underbrace{\int_{\partial U} \Delta w \nabla\psi \cdot dS}_{=0}\end{aligned}$$

and

$$\begin{aligned}\iint_U \psi \Delta\chi_{A^e} &= -\iint_U \nabla\psi \cdot \nabla(\chi_{A^e}) + \underbrace{\int_{\partial U} \psi \nabla(\chi_{A^e}) \cdot dS}_{=0} \\ &= \iint_U \chi_{A^e} \Delta\psi - \int_{\partial U} \chi_{A^e} \nabla\psi \cdot dS \\ &= \iint_{A^e} \Delta\psi - \underbrace{\int_{\partial U} \chi_{A^e} \nabla\psi \cdot dS}_{=0}.\end{aligned}$$

Hence the weak form of (1.7) can be written as

$$\iint_U \Delta w \Delta\psi + \frac{\alpha c}{D} \iint_{S^e} \Delta w \iint_{A^e} \Delta\psi = \sigma \iint_U w\psi, \qquad \forall \psi \in H_0^1(U) \cap H^2(U).$$

Assume throughout this paper that $A^e = S^e$ so that the bilinear form on the left-hand side is positive and symmetric, and positive real eigenvalues can be expected. On the other hand, the Fredholm Alternative holds due to the compact embedding of $H_0^1(U) \cap H^2(U)$ into $L^2(U)$. This fact will be used in the later derivation of the functional differential.

2. Level set formulation. An integral equation approach for the analytical solution to the corresponding one dimensional eigenvalue problem (1.7) was first proposed in [17] and generalized to the two dimensional case in [4]. Shape optimization in two dimensions was studied in [20] using boundary parameterization optimization. In order to handle more general patch geometries, we use the level set method for optimization problems introduced in [11, 15]. The applications of the level set method to other type of structural boundary design problems can be found in [16].

A key idea is to represent the unknown set A^e as the level set of a scalar function $\phi(x)$, where

$$\phi(x) \begin{cases} > 0 & \text{inside } A^e \\ = 0 & \text{on } \partial A^e \\ < 0 & \text{outside } A^e. \end{cases} \tag{2.1}$$

The generic optimization problem can now be reformulated as

$$\text{minimize} \quad F[\phi] \quad \text{subject to } G(\phi) = 0$$

where F is the minimum vibration frequency in terms of the level set function and G can be written as

$$G(\phi) = \iint_{\{x:\phi>0\}} dx - K. \tag{2.2}$$

The Lagrange multiplier method can be used to solve the constrained optimization problem. Let γ be the Lagrange multiplier, then the augmented optimization problem can be written as

$$L(\phi, \gamma) = F(\phi) + \gamma G(\phi).$$

The necessary condition for ϕ to be a minimizer is

$$D_\phi L(\phi, \gamma) = D_\phi F(\phi) + \gamma D_\phi G(\phi) = 0. \tag{2.3}$$

Combining (2.3) and (2.2) we can in principle determine ϕ and γ. Numerically, we start from an initial guess of the boundary of A^e and keep updating it following the gradient direction until the algorithm converges.

To determine the gradient along the level curve, We compute $D_\phi F$ and $D_\phi G$ in terms of ϕ as follows:

- Compute the shape derivative of F.

  Assume σ solves (1.7) with the corresponding eigenfunction w. Let σ_δ and w_δ be the variation in σ and w with respect to the variation in A^e, respectively. The variation in A^e is the symmetric difference between two different sets which will be denoted by "diff" in the following presentation. Since both of the pairs (σ, w) and $(\sigma + \sigma_\delta, w + w_\delta)$ satisfy the above eigenvalue problem, we have

$$\begin{aligned}&\Delta^2 w_\delta + \beta \left(\iint_{A^e} \Delta w_\delta \right) \Delta \chi_{A^e} - \sigma w_\delta \\ &= \sigma_\delta w - \beta \left(\iint_{A^e} \Delta w \right) \Delta \chi_{\text{diff}} - \beta \left(\iint_{\text{diff}} \Delta w \right) \Delta \chi_{A^e}\end{aligned}$$

  where $\beta = \frac{\alpha c}{D}$.

  By Fredholm Alternative, for the above equation of w_δ to yield a nontrivial solution, the right-hand side must be orthogonal to w, which implies that

$$\sigma_\delta = \frac{2\beta \iint_{A^e} \Delta w \iint_{\text{diff}} \Delta w}{\iint_U w^2}. \tag{2.4}$$

  Let δx denote the infinitesimal displacement of a point $x \in \partial A^e$ under the variation of A^e. As explained in [11, 15], if ∂A^e is smooth, then for any scalar function $f(x)$,

$$\iint_{\text{diff}} f = -\int_{\partial A^e} \delta x \cdot \frac{\nabla \phi}{|\nabla \phi|} f. \tag{2.5}$$

  Note that δx is a function of $x \in \partial A^e$ so the line integral on the right over ∂A^e makes sense. In addition, by the definition of the level set function ϕ,

$-\frac{\nabla\phi}{|\nabla\phi|}$ is the outer normal of the patch boundary. Therefore, (2.4) amounts to

$$\sigma_\delta = -\frac{2\beta \iint_{A^e} \Delta w \int_{\partial A^e} \delta x \cdot \frac{\nabla\phi}{|\nabla\phi|} \Delta w}{\iint_U w^2}. \tag{2.6}$$

- Represent the shape derivatives $D_\phi F$ and $D_\phi G$ in terms of the level set function ϕ.

  Let $\delta\phi$ be the infinitesimal variation of the level set function ϕ under the variation of A^e. In order to rewrite σ_δ in terms of $\delta\phi$, we take the variation of $\phi(x) = 0$, which yields the time-discretized Hamilton-Jacobi equation

$$\delta\phi + \nabla\phi \cdot \delta x = 0 \tag{2.7}$$

  and allows us to represent the directional derivative of F as

$$D_\phi F \cdot \delta\phi = \sigma_\delta = \frac{2\beta \iint_{A^e} \Delta w \int_{\partial A^e} \frac{\delta\phi}{|\nabla\phi|} \Delta w}{\iint_U w^2}. \tag{2.8}$$

  Similarly by (2.5) and (2.7), the directional derivative of G reads

$$D_\phi G \cdot \delta\phi = \int_{\partial A^e} \frac{\delta\phi}{|\nabla\phi|}. \tag{2.9}$$

- Determine the gradient along ∂A^e.

  We use the projected gradient method introduced in [11, 15] to determine the gradient along ∂A^e.
  To view the varying patch boundary in a continum framework, we assume that it is driven by some vector field. The evolving rate of ∂A^e at each point x is just δx, which can be understood as the rate of change of the displacement with respect to the patch shape.
  Let v be the normal component of δx on ∂A^e, i.e.

$$v = \delta x \cdot \frac{\nabla\phi}{|\nabla\phi|}.$$

  Then the time-discretized Hamilton-Jacobi equation (2.7) can be written equivalently as

$$\delta\phi + v|\nabla\phi| = 0. \tag{2.10}$$

  By (2.8),(2.9) and (2.10), we have

$$\begin{aligned} D_\phi L \cdot \delta\phi &= D_\phi F \cdot \delta\phi + \gamma D_\phi G \cdot \delta\phi \\ &= \int_{\partial A^e} \frac{\delta\phi}{|\nabla\phi|} \left(\gamma + \frac{2\beta \iint_{A^e} \Delta w}{\iint_U w^2} \Delta w \right) \\ &= -\int_{\partial A^e} v \left(\gamma + \frac{2\beta \iint_{A^e} \Delta w}{\iint_U w^2} \Delta w \right). \end{aligned}$$

Hence, to minimize $D_\phi L \cdot \delta\phi$, a descent direction can be chosen as

$$v = \frac{2\beta \iint_{A^e} \Delta w}{\iint_U w^2} \Delta w + \gamma. \tag{2.11}$$

To determine the Lagrange multiplier, we use the projection approach presented in [11] basing on the one introduced in [14].
Differentiating the constraint $G(\phi) = 0$ yields

$$D_\phi G \cdot \delta\phi = 0,$$

which is, by (2.9) and (2.10)

$$\int_{\partial A^e} \frac{\delta\phi}{|\nabla\phi|} = \int_{\partial A^e} v = 0.$$

Since

$$0 = \int_{\partial A^e} v = \int_{\partial A^e} vn \cdot n = -\int_{\partial A^e} v \frac{\nabla\phi}{|\nabla\phi|} \cdot n = -\iint_{A^e} \nabla \cdot \left(v \frac{\nabla\phi}{|\nabla\phi|} \right),$$

we conclude by (2.11) that

$$\gamma = -\frac{2\beta \iint_{A^e} \Delta w}{\iint_U w^2} \cdot \frac{\iint_{A^e} \nabla \cdot \left(\Delta w \frac{\nabla\phi}{|\nabla\phi|} \right)}{\iint_{A^e} \nabla \cdot \frac{\nabla\phi}{|\nabla\phi|}}. \tag{2.12}$$

3. The numerical scheme. The main algorithm for the optimization is shown in the following:

initialize $\phi(x)$
do while $D_\phi L \neq 0$
solve for the eigenvalue σ *and the corresponding eigenvector* w
compute the Lagrange multiplier γ *using (2.12)*
compute the descent direction v *(2.11)*
update ϕ *via the time-discretized Hamilton-Jacobi equation (2.10)*

Note that the eigenvalue and the corresponding eigenvector are to be computed at each step. We achieve this by the integral equation approach presented in [20], where the eigenvalue problem (1.4) is converted into an integral equation which is furthermore approximated by a finite dimensional linear system. The procedure goes as follows:

- Convert the PDE into an integral equation with an explicit kernel.

Let $K(x, y; x_1, y_1) = g(x, y; x_1, y_1) + p(x, y)q(x_1, y_1)$, where

$$g(x, y; x_1, y_1) = \sum_{m=1}^{\infty} \sum_{n=1}^{\infty} \frac{4}{ab} g_{mn} \sin\frac{m\pi x}{a} \sin\frac{n\pi y}{b} \sin\frac{m\pi x_1}{a} \sin\frac{n\pi y_1}{b}$$

with $g_{mn} = \frac{1}{\pi^4 \omega_{mn}^2}$ and $\omega_{mn} = \left(\frac{m}{a}\right)^2 + \left(\frac{n}{b}\right)^2$,

$$p(x,y) = \iint_{A^e} \Delta g(x,y;x_1,y_1)\,dx_1\,dy_1$$

and

$$q(x_1,y_1) = -cC_q \iint_{S^e} \Delta g(x,y;x_1,y_1)\,dx\,dy$$

with

$$C_q = \frac{\alpha}{D + \alpha c|A^e|}.$$

Note that $g(x,y;x_1,y_1)$ is the kernel of the biharmonic operator with the simply supported boundary conditions, i. e. it satisfies

$$\begin{cases} \Delta^2 g = \delta(x-x_1)\delta(y-y_1) & \text{in } U \\ g(x,y;x_1,y_1) = 0 & \text{on } \partial U \\ g_{xx}(0,y;x_1,y_1) = g_{xx}(a,y;x_1,y_1) = 0 & \text{for } 0 < y < b \\ g_{yy}(x,0;x_1,y_1) = g_{yy}(x,b;x_1,y_1) = 0 & \text{for } 0 < x < a \end{cases} \tag{3.1}$$

where $\delta(x)\delta(y)$ denotes the Dirac measure giving unit mass at the origin. And $p(x,y)$ solves

$$\begin{cases} \Delta^2 p = \Delta\chi_{A^e} & \text{in } U \\ p(x,y) = 0 & \text{on } \partial U \\ \dfrac{\partial^2 p}{\partial n^2} = 0 & \text{on } \partial U. \end{cases} \tag{3.2}$$

Then (1.4) implies that

$$w(x,y) = \sigma \iint_U K(x,y;x_1,y_1) w(x_1,y_1)\,dx_1\,dy_1. \tag{3.3}$$

- Approximate the integral equation by a finite dimensional linear system.

Define

$$\varphi_{mn}(x,y) = \frac{2}{\sqrt{ab}} \sin\frac{m\pi x}{a} \sin\frac{n\pi y}{b} \quad \text{for } m,n = 1,2,\cdots.$$

$\{\varphi_{mn}(x,y)\}$ forms a complete orthonormal system in the function space $L^2([0,a]\times[0,b])$ with simply supported boundary conditions, which the functions $w(x,y)$, $p(x,y)$ and $q(x,y)$ all belong to.
Denote d_{mn}, p_{mn} and q_{mn} as the Fourier coefficients of the functions $w(x,y)$, $p(x,y)$ and $q(x,y)$, respectively, for $m,n = 1,2,\cdots$. That is,

$$d_{mn} = \iint_U w(x,y)\varphi_{mn}(x,y)\,dx\,dy,$$

$$p_{mn} = \iint_U p(x,y)\varphi_{mn}(x,y)\,dx\,dy$$

and

$$q_{mn} = \iint_U q(x,y)\varphi_{mn}(x,y)\,dx\,dy.$$

Also put

$$Q = \iint_U q(x,y)w(x,y)\,dx\,dy$$

and

$$R = \iint_U p(x,y)q(x,y)\,dx\,dy.$$

Set $\mu = \frac{1}{\sigma}$ for $\sigma \neq 0$. Substituting $w(x,y) = \sum_{m=1}^{\infty}\sum_{n=1}^{\infty} d_{mn}\varphi_{mn}(x,y)$ into equation (3.3) yields

$$\mu \sum_{m=1}^{\infty}\sum_{n=1}^{\infty} d_{mn}\varphi_{mn}(x,y) = \sum_{m=1}^{\infty}\sum_{n=1}^{\infty} g_{mn}d_{mn}\varphi_{mn}(x,y) + Qp(x,y). \tag{3.4}$$

(1) Multiplying equation (3.4) by $\varphi_{kl}(x,y)$ and integrating both sides over U yields

$$\mu d_{kl} = g_{kl}d_{kl} + p_{kl}Q. \tag{3.5}$$

for $k,l = 1,2,\cdots$.

(2) Multiplying equation (3.4) by $q(x,y)$ and integrating both sides over U yields

$$\mu Q = \sum_{m=1}^{\infty}\sum_{n=1}^{\infty} g_{mn}q_{mn}d_{mn} + RQ. \tag{3.6}$$

(3) Formally define the infinite dimensional matrix B as

$$B = \begin{pmatrix} \overline{G} & G_c \\ G_r & R \end{pmatrix},$$

where $\overline{G}$ is the infinite diagonal matrix

$$\overline{G} = \operatorname{diag}(g_{11}, g_{12}, \ldots, \ldots)$$

and G_c, G_r are the infinite column vector and the infinite row vector, respectively,

$$G_c = (p_{11}, p_{12}, \ldots, \ldots)^T \quad \text{and} \quad G_r = (g_{11}q_{11}, g_{12}q_{12}, \ldots, \ldots).$$

Combining (3.5) and (3.6), we get

$$Bv = \mu v, \qquad v = (d_{11}, d_{12}, \ldots, Q).$$

- Finite dimensional approximation of the infinite linear system.

  Truncating the first MN terms of the Green's function $g(x,y;\xi,\eta)$:

$$g^{MN}(x,y;\xi,\eta)=\sum_{m=1}^{M}\sum_{n=1}^{N}g_{mn}\varphi_{mn}(x,y)\varphi_{mn}(\xi,\eta),$$

  the above infinite linear system can be approximated by $MN+1$ linear equations (a finite dimensional eigenvalue problem):

$$B^{MN}v^{MN}=\mu^{MN}v^{MN},\quad \text{for } v^{MN}=(v_1,v_2,\cdots,v_{MN+1}),$$

  with B^{MN} defined as an $(MN+1)\times(MN+1)$ matrix:

$$B^{MN}=\begin{pmatrix}\overline{G}^{MN} & G_c^{MN}\\ G_r^{MN} & R\end{pmatrix},$$

  where

$$\overline{G}^{MN}=\operatorname{diag}(b_{11},b_{22},\cdots,b_{MN,MN}),$$

$$G_c^{MN}=(b_{1,MN+1},b_{2,MN+1},\cdots,b_{MN,MN+1})^T,$$

$$G_r^{MN}=(b_{MN+1,1},b_{MN+1,2},\cdots,b_{MN+1,MN})$$

  and

$$R=b_{MN+1,MN+1}.$$

  Although it is hard to give a rigid error estimate for the convergence rate of the approximated solution, the above approximation is numerically convincing as shown later.

- Explicit formulations of p_{mn}, q_{mn} and R.

  We shall express p_{mn}, q_{mn} and R explicitly in order to determine the matrix B. By the definitions above, we have

$$\begin{aligned}
p_{mn}&=\iint_U p(x,y)\varphi_{mn}(x,y)\,dx\,dy\\
&=\iint_U \varphi_{mn}(x,y)\left(\iint_{A^e}\Delta g(x,y;x_1,y_1)\,dx_1\,dy_1\right)dx\,dy\\
&=-\iint_U \varphi_{mn}(x,y)\left(\iint_{A^e}\sum_{k=1}^{\infty}\sum_{l=1}^{\infty}\hat{g}_{kl}\varphi_{kl}(x,y)\varphi_{kl}(x_1,y_1)\,dx_1\,dy_1\right)dx\,dy\\
&=-\sum_{k=1}^{\infty}\sum_{l=1}^{\infty}\hat{g}_{kl}\left(\iint_U\varphi_{kl}(x,y)\varphi_{mn}(x,y)\,dx\,dy\right)\left(\iint_{A^e}\varphi_{kl}(x_1,y_1)\,dx_1\,dy_1\right)\\
&=-\hat{g}_{mn}\iint_{A^e}\varphi_{mn}(x_1,y_1)\,dx_1\,dy_1,
\end{aligned}$$

$$q_{mn} = c_0 C_q \hat{g}_{mn} \iint_{S^e} \varphi_{mn}(x,y)\, dx\, dy$$

and

$$R = \sum_{m=1}^{\infty} \sum_{n=1}^{\infty} p_{mn} q_{mn}.$$

REMARK 3.1. The advantage of the integral approach for the eigenvalue problem is that the size of the linear system does NOT depend on the mesh size. Since computing the eigenvalue and the eigenvector is the key time-consuming issue in this numerical scheme, the mesh independence of the matrix size allows us to refine the mesh without dramatically slowing down the computational process. Actually, the choice of $M, N = 5$ is large enough to provide very accurate results of the eigenvalue and the eigenvector.

4. Numerical results. Numerical simulations are provided in this section.

To update the level set function, higher order schemes such as ENO [13] and WENO [7] are advanced schemes for solving Hamilton-Jacobi equations. With an acceptable accuracy, we simply implement the monotone upwind scheme [12] here. Moreover, we do not use the reinitialization technique [18] which would have also increased the computational stability.

For a numerical test, we consider a square domain $U = (0,1)\times(0,1)$ and discretize it using regular meshes. The physical constants are taken as follows:

$$\rho = 1.19, \quad h = 0.0016, \quad D = 1.167, \quad c = 28.1895 \quad \text{and} \quad \alpha = 1.64 \times 10^{-4}.$$

Our numerical results show that the minimizer of the optimization problem is NOT sensitive to the initial choice of the patch shape, which provides positive evidence of the uniqueness of the minimizer.

The following types of initial data are tested (the region occupied by the patch is in white):

(1) A square patch located in the center of the plate with boundaries

$$|x - 0.5| = 0.4\sqrt{\pi}/2, \quad |y - 0.5| = 0.4\sqrt{\pi}/2.$$

Taking the mesh size of $\Delta x = \Delta y = 1/80$ (80×80 grids), Figure 1 shows the evolution of the square patch towards the optimal shape and Figure 2 shows the minimum vibration frequency as a function of the number of iterations.

(2) A circular patch located in the center of the plate with boundary

$$(x - 0.5)^2 + (y - 0.5)^2 = 0.4^2.$$

Taking the mesh size of $\Delta x = \Delta y = 1/100$ (100×100 grids), Figure 3 shows the evolution of the circular patch towards the optimal shape and Figure 4 shows the minimum vibration frequency as a function of the number of iterations.

(3) A polygonal patch located in the center of the plate with boundary

$$|x + y - 0.5| = 0.4\sqrt{\pi/2}, \quad |y - 0.5| = 0.4\sqrt{\pi/2}.$$

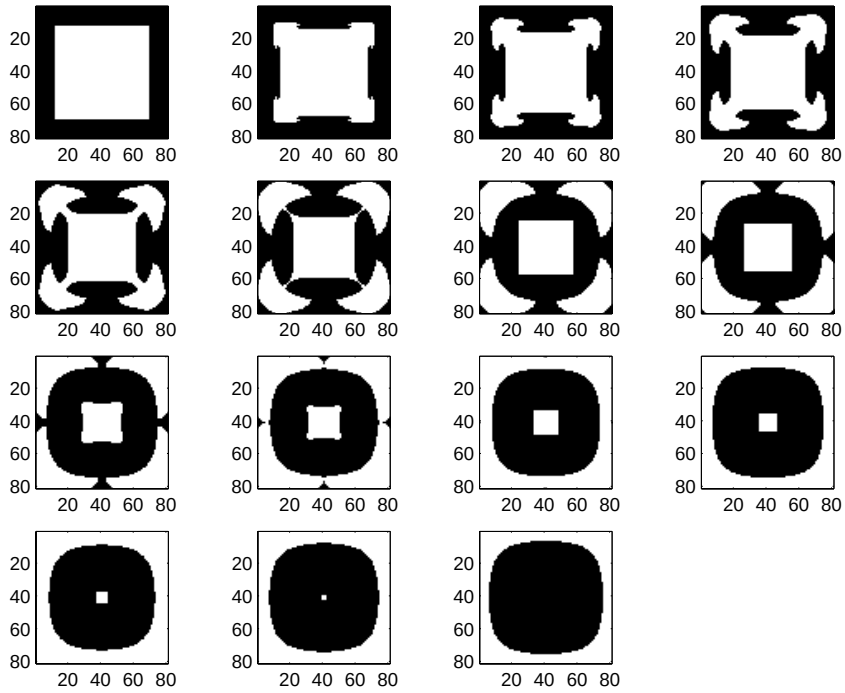

FIG. 1. *Shape evolution of the square patch*

Taking the mesh size of $\Delta x = \Delta y = 1/100$ (100×100 grids), Figure 5 shows the evolution of the polygonal patch towards the optimal shape and Figure 6 shows the minimum vibration frequency as a function of the number of iterations.

The above choices of the patch size make the patch areas the same in all cases. We observe from the following numerical results that the three different initial data lead to the same minimum value of the minimum vibration frequency. In addition, the minimizers in the three cases are quite similar (in the sense that they all break down into pieces first and evolve towards the boundary).

(4) Two circular patches of radius 0.2 located in the center of the upper half plate and the center of the lower half plate, respectively.

Taking the mesh size of $\Delta x = \Delta y = 1/100$ (100×100 grids), Figure 7 shows the evolution of the two circular patches towards the optimal shape and Figure 8 shows the minimum vibration frequency as a function of the number of iterations.

(5) Two square patches of length $0.2 \times \sqrt{\pi}$ located in the center of the upper half plate and the center of the lower half plate, respectively.

Taking the mesh size of $\Delta x = \Delta y = 1/100$ (100×100 grids), Figure 9 shows the evolution of the two square patches towards the optimal shape and Figure 10 shows the minimum vibration frequency as a function of the number of iterations.

In Case (4) and (5), the patch regions still evolve towards the plate boundary but keep their original connectivity without merging into one piece in the end.

REMARK 4.1. Here is an interesting phenomenon: Comparing with the patch

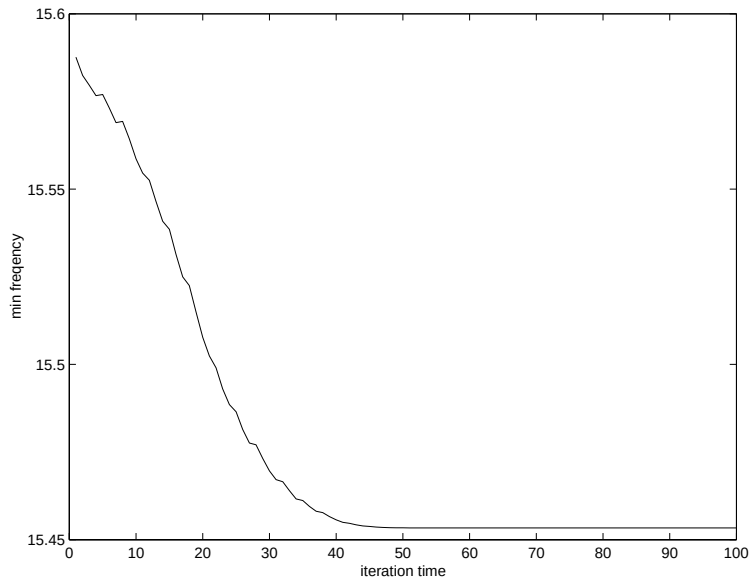

FIG. 2. *Minimum vibration frequency λ vs. iteration number for the square patch*

behaviors in Case (4) and (5), although the patches in Case (1), (2) and (3) lose their original connectivity during the evolution, each ends up in a single piece. We believe that the center patch regions in Case (1), (2) and (3) play an important role in their final unification.

Due to the numerical diffusion, the patch area may dissipate during the iteration. This can be solved by modifying the Lagrange multiplier γ using Newton's method as stated in [11]. We do not implement it here since only slight area dissipation occurs in our computation and it does not affect the property of the minimizer.

5. Discussions. The level set method is implemented for the shape optimization of plate piezoelectric patches. It is proved to be quite efficient for the presented problem in which complicated topological changes occur during the evolution of the free boundary. On the other hand, the integral equation approach introduced in [4, 17, 20] is used to speed up the computation of the corresponding eigenvalue problem at each iteration step.

According to the numerical simulation, the optimal shape of the patch, does not seem to depend on the initial data (with the same connectivity), which provides positive evidence of the uniqueness of the minimizer of the optimization problem (with the same connectivity). We conclude that to minimize the minimum vibration frequency, the patch has the tendency to evolve towards the plate boundary. By choosing the positive gradient direction, we can do the same work to maximize the minimum vibration frequency. And a polygonal shape located in the patch center is a preferred maximizer and the numerical results also give positive evidence of its uniqueness.

The assumption that $A^e = S^e$ is made in this paper not only for the simplification but also for the mathematical rigidity of the problem, since it has not been proved theoretically that the eigenvalue problem studied above has real and positive minimum eigenvalue when $A^e \neq S^e$, although numerical results in [21, 20] provide a positive

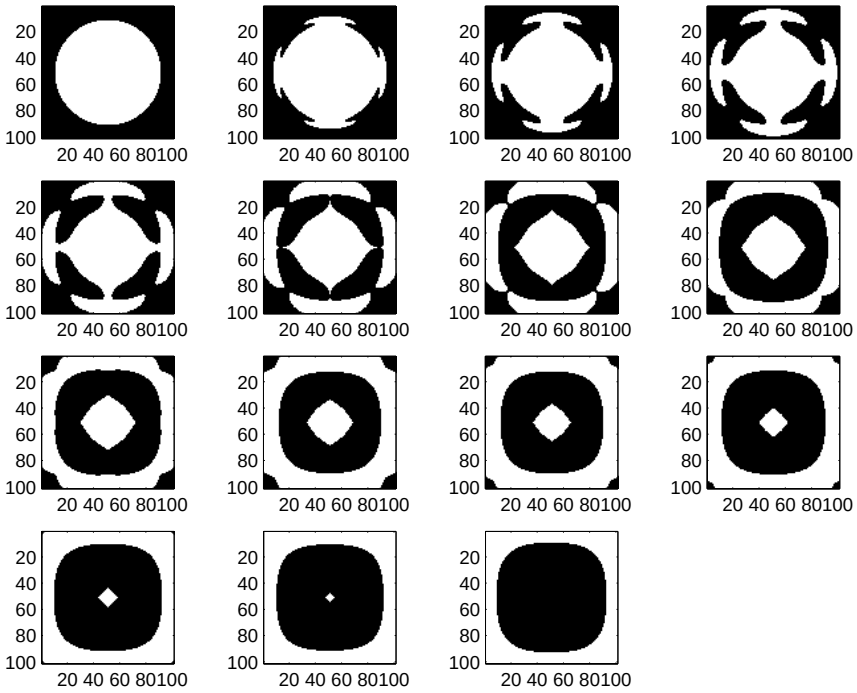

FIG. 3. *Shape evolution of the circular patch*

answer in several cases. However, the level set formulation and the integral equation approach introduced here can be easily extended to the general case when $A^e \neq S^e$.

Acknowledgments. This paper was partially completed during the author's stay at Institute for Pure and Applied Mathematics, UCLA. It is a privilege to meet Professor Stanley Osher and this work was the result of valuable conversations with him. The author would like to thank him for all the help and enlightening guidance. The author would also like to thank Professor John Bruch and Professor James Sloss at UCSB for great help with the integral equation approach, and to thank Chiu-Yen Kao and Bing Song at UCLA for helpful discussions on the numerics.

REFERENCES

[1] G. ALLAIRE, F. JOUVE & A.-M. TOADER, *Structural optimization by the level set method*, CMAP, Ecole Polytechnique Report 2002.

[2] R. BARBONI, A. MANNINI, E. FANTINI & P. GAUDENZI, *Optimal placement of PZT actuators for the control of beam dynamics*, Smart Materials and Structures, 9 (2000), pp. 110–120.

[3] J. C. BRUCH, JR., J. M. SLOSS, S. ADALI & I. S. SADEK, *Optimal piezo-actuator locations/lengths and applied voltage for shape control of beams*, Smart Materials and Structures, 9 (2000), pp. 205–211.

[4] J. C. BRUCH, JR., J. M. SLOSS, I. S. SADEK & S. ADALI, *Analytical solution technique for plate-patch piezoelectric sensor-actuator vibration control problems*, Proceedings of SPIE, Smart Structures and Materials 2002, Modeling, Signal Processing and Control, March 18-21, 2002, San Diego, CA, 4693, pp. 104–111.

[5] R. L. CLARK & C. R. FULLER, *Experiments on active control of structurally radiated sound using multiple piezoelectric actuators*, Journal of Acoustical Society of America, 91 (1992),

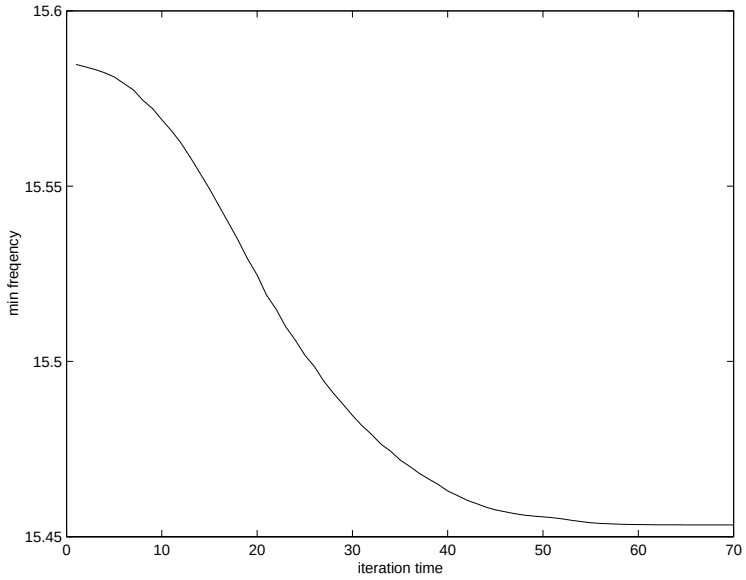

FIG. 4. *Minimum vibration frequency λ vs. iteration number for the circular patch*

pp. 3313–3320.

[6] C. Y. HSU, C. C. LIN & L. GAUL, *Vibration and sound radiation controls of beams using layered modal sensors and actuators*, Smart Materials and Structures, 7 (1998), pp. 446–455.

[7] G. JIANG & D. PENG, *Weighted ENO schemes for Hamilton-Jacobi equations*, SIAM J. Sci. Comput., 21 (2000), pp. 2126–2143.

[8] D. B. KOCONIS, L. P. KOLLAR & G. S. SPRINGER, *Shape control of composite plates and shells with embedded actuators. II. Desired shape specified*, Journal of Composite Materials, 28 (1994), pp. 459–482.

[9] C. C. LIN & H. N. HUANG, *Vibration control of beam-plates with bonded piezoelectric sensors and actuators*, Computers and Structures, 73 (1999), pp. 239–248.

[10] S. NA & L. LIBRESCU, *Oscillation control of cantilevers via smart materials technology and optimal feedback control: actuator location and power consumption issues*, Smart Materials and Structure, 9 (1998), pp. 833–842.

[11] S. OSHER & F. SANTOSA, *Level set methods for optimization problems involving geometry and constraints: I. Frequencies of a two-density inhomogeneous drum*, Journal of Computational Physics, 171 (2001), pp. 272–288.

[12] S. OSHER & J. SETHIAN, *Fronts propagating with curvature-dependent speed: algorithms based on Hamilton-Jacobi formulations*, Journal of Computational Physics, 79 (1988), pp. 12–49.

[13] S. OSHER & C. SHU, *High order essentially nonoscillatory schemes for Hamilton-Jacobi equations*, SIAM J. Numer. Anal., 28 (1991), pp. 907–922.

[14] L. RUDIN, S. OSHER & E. FATEMI, *Nonlinear total variation based noise removal algorithms*, Physica D, 60 (1992).

[15] F. SANTOSA, *A level-set approach for inverse problems involving obstacles*, Control, Optimization and Calculus of Variation, 1 (1996), pp. 17–33.

[16] J. SETHIAN & S. WIEGMANN, *Structural boundary design via level set and immersed interface methods*, J. Comput. Phys., 163:2 (2000), pp. 489–528.

[17] J. M. SLOSS, J. C. BRUCH, JR., S. ADALI & I. S. SADEK, *Piezoelectric patch control using an integral equation approach*, Thin-Walled Structures, 39 (2001), pp. 45–63.

[18] M. SUSSMAN, P. SMEREKA & S. OSHER, *A level set approach for computing solutions to incompressible two-phase flow*, J. Comput. Phys., 114 (1994), pp. 146–159.

[19] H. S. TZOU, *A new distributed sensation and control theory for intelligent shells*, Journal of Sound and Vibration, 153:2 (1992), pp. 335–350.

[20] J. ZHANG, Ph.D. thesis, UCSB, 2002.

[21] J. ZHANG, J. C. BRUCH, JR. & J. M. SLOSS, *An integral equation approach for shape optimization of plate piezoelectric patches*, accepted by Journal of Vibration and Control.

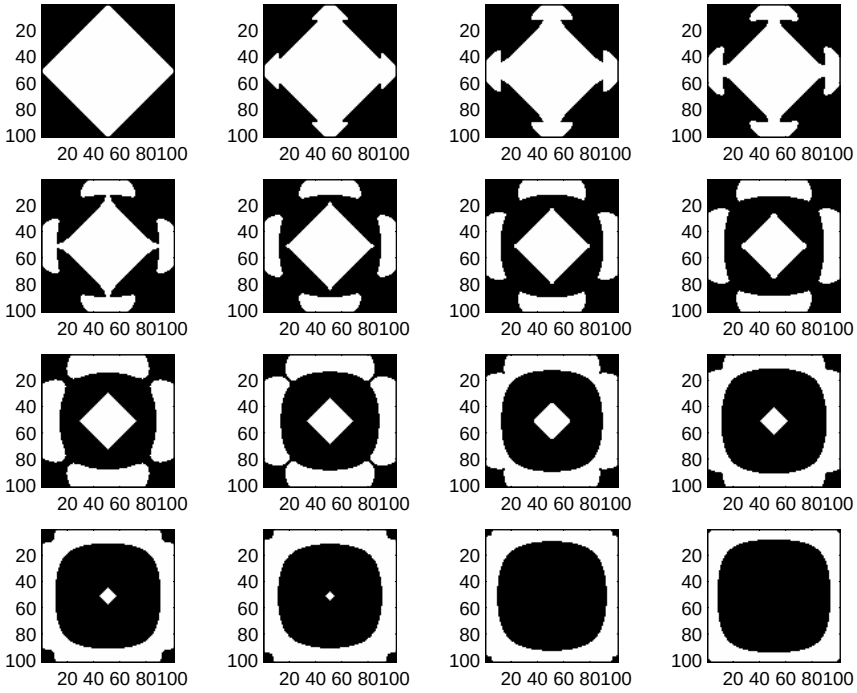

FIG. 5. *Shape evolution of the polygonal patch*

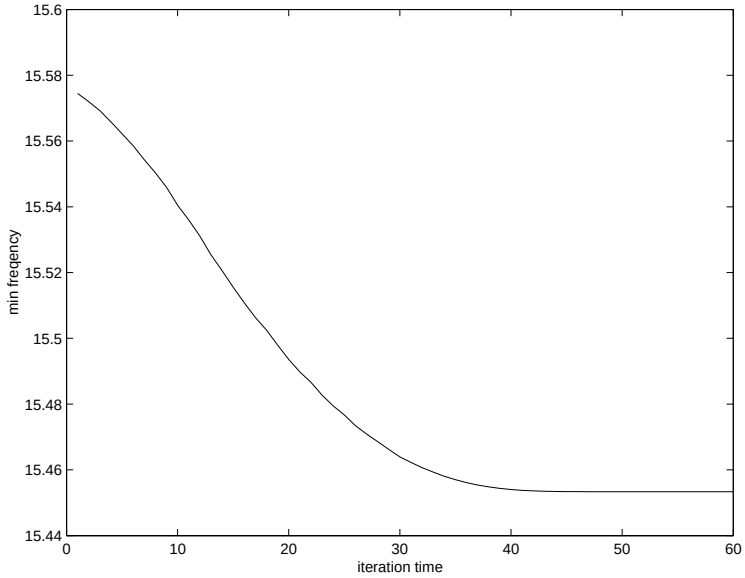

FIG. 6. *Minimum vibration frequency λ vs. iteration number for the polygonal patch*

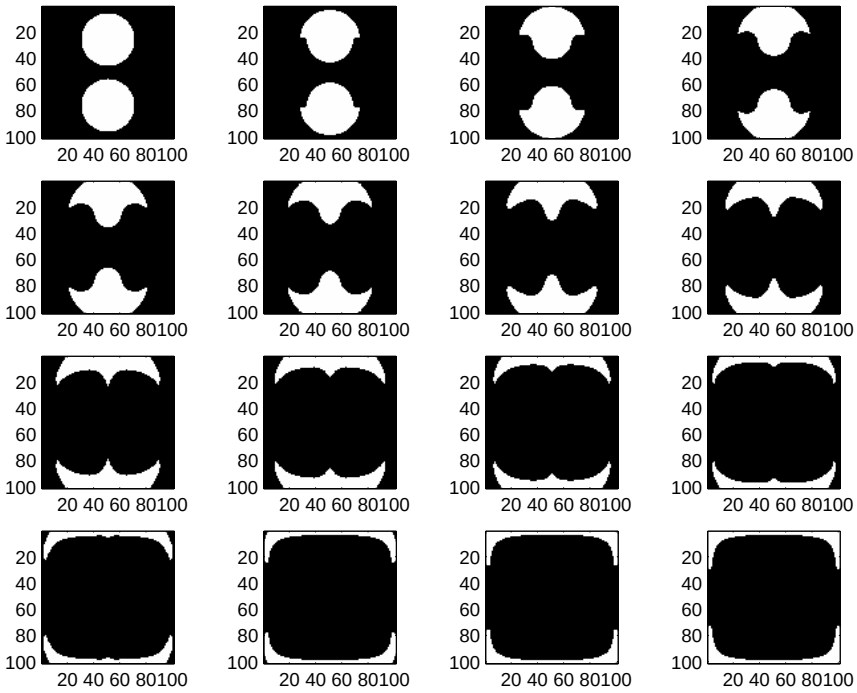

FIG. 7. *Shape evolution of two circular patches*

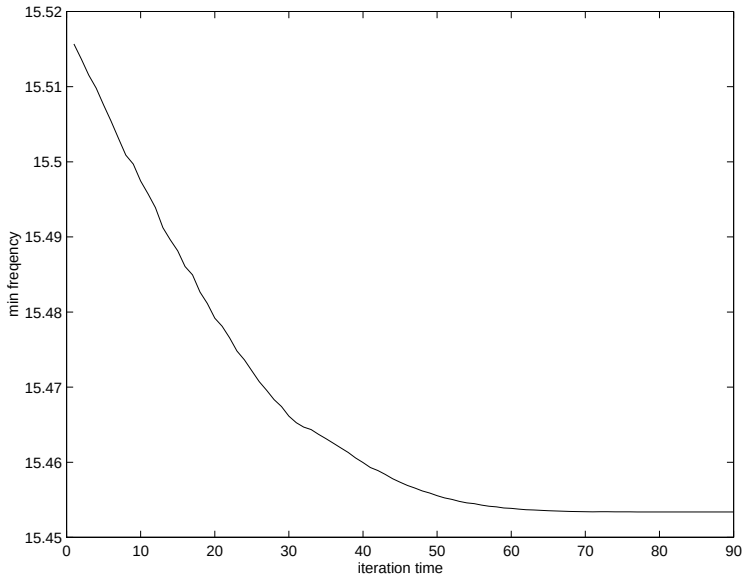

FIG. 8. *Minimum vibration frequency λ vs. iteration number for two circular patches*

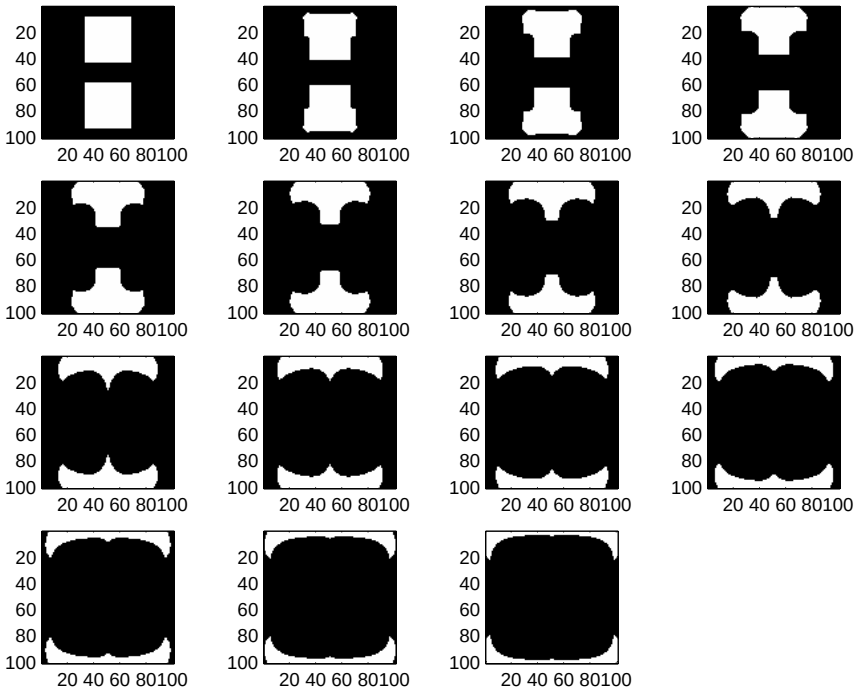

FIG. 9. *Shape evolution of two square patches*

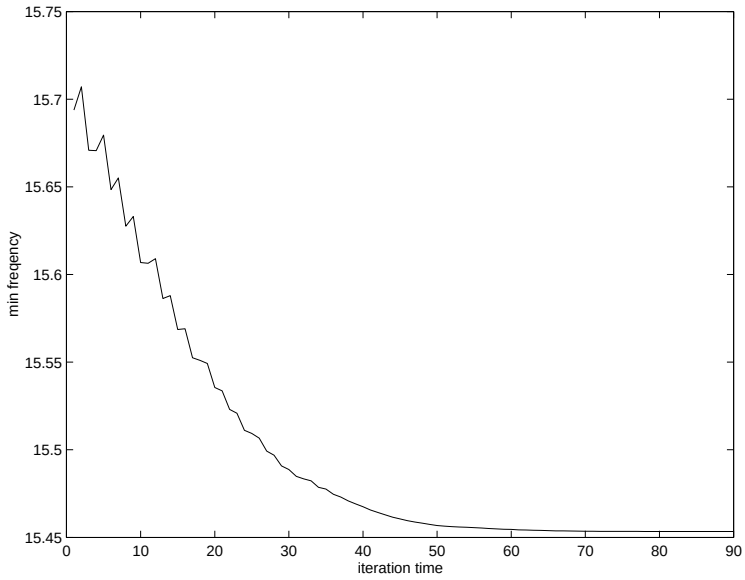

FIG. 10. *Minimum vibration frequency λ vs. iteration number for two square patches*